Journal of Communications Technology and Electronics, Vol. 42, No. 4, 1997, pp. 469–474. Translated from Radiotekhnika i Elektronika, Vol. 42, No. 4, 1997, pp. 506–512.

NOVEL RADIO SYSTEMS AND ELEMENTS

Magnetic Induction Tomography

A. V. Korzhenevskii and V. A. Cherepenin

Received September 30, 1996

Abstract—The principles underlying the operation of the magnetic-induction tomograph are examined. The possibility is shown to exist of independently reconstructing the distributions of conductivity and permittivity inside an object as it is explored by an alternating magnetic field. Some of the likely configurations for the measuring system of a magnetic-induction tomograph, an image reconstruction algorithm, and applications of magnetic-induction tomography are discussed.

INTRODUCTION

Computerized tomography that utilizes X-rays or nuclear magnetic resonance (NMR tomography) is being widely used in medicine and industry. In the wider sense, computerized tomography has as its basis the possibility of mathematically reconstructing the spatial distribution of some characteristic of the material inside an object from how this material affects the physical field or radiation that threads the object and is picked up by external detectors [1].

Recently, new tomographic techniques have been proposed, in which the exploring signal is an alternating electric current or an electromagnetic field. The most successful of them has been electric-impedance or applied-potential tomography [2]. Its rationale is as follows: a weak alternating electric current is passed through the conducting object of interest (in medicine, this would be the patient's body) using electrodes applied to its surface. As a result, potentials arise on the surface, and these are picked off and measured via other (or, sometimes, the same) electrodes. With a set of linearly independent measurements taken by different combinations of injecting and sensing electrodes, it is possible to reconstruct the distribution of the electric impedance inside the object.

Quite a number of techniques have been devised to solve the inverse problem for the case in question. However, tomographs in actual service most often use the method of back projection along the equipotential lines of the electric field [2], similar to traditional tomography. With this approach, it is possible to visualize only small variations of conductivity inside the object and there is also a need for a reference set of data representing the initial conductivity. This has come to be known as dynamic visualization. In [3] and [4], a modified back-projection method is proposed for electric-impedance tomography. It offers a way to obtain images of static objects in the human body through the use of a synthesized set of reference data corresponding to a body with a homogeneous conductivity and enables this form of electric-impedance tomography to be used in medical practice [5].

Special promise for tomography is held by high-frequency magnetic fields, notably, their interaction with a conducting medium where they give rise to displacement currents. In [6] and [7], attempts were made to utilize such interaction in order to visualize conductivity, but the empirical approach used there failed to yield satisfactory results. The aim of this paper is to elucidate the physical principles underlying magnetic-induction tomography and to formulate, on basis of these principles, approaches to the design of workable devices and image reconstruction algorithms.

1. THE PHYSICAL MODEL AND SOLUTION OF THE INVERSE PROBLEM

Let there be a source (inductor) and a sink (detector) of an alternating magnetic field spaced some distance apart. These may, for example, be two identical inductively coupled turns (Fig. 1). One will act as an inductor connected to a source of ac voltage U_i at frequency ω, such that $U_i = U_1\cos(\omega t)$. The other will act as a detector connected to an instrument measuring the emf induced in it. The electromagnetic field filled by an inhomogeneous medium can be described by Maxwell's equations, which in the case at hand may conveniently be written as

$$\nabla^2\mathbf{A} + \nabla\ln\mu\times(\nabla\times\mathbf{A}) - \frac{4\pi\mu}{c}\left(\sigma+\frac{i\omega}{4\pi}\varepsilon\right)\left(\nabla\varphi+\frac{i\omega}{c}\mathbf{A}\right) = 0,$$

$$\nabla^2\varphi + \nabla\ln\left(\sigma+\frac{i\omega}{4\pi}\varepsilon\right)\left(\nabla\varphi+\frac{i\omega}{c}\mathbf{A}\right) = 0, \qquad (1)$$

$$\nabla\cdot\mathbf{A} = 0,$$

$$\mathbf{B} = \nabla\times\mathbf{A}, \quad \mathbf{E} = -\nabla\varphi - \frac{i\omega}{c}\mathbf{A},$$

where $\mathbf{A}$ is the magnetic vector potential, φ is

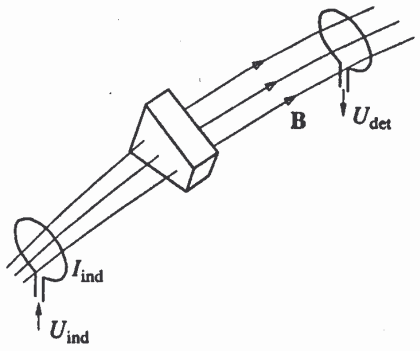

Fig. 1. Measuring system of a magnetic-induction tomograph.

the electrostatic scalar potential (the Coulomb calibration, div$\mathbf{A} = 0$, is used), $\mathbf{E}$ is the electric field intensity, $\mathbf{B}$ is the magnetic induction, μ is the permeability, ε is the permittivity, σ is the specific conductivity of the medium, and c is the velocity of light. The first of the above equations corresponds to Maxwell's equation for rot$(\mathbf{B}/\mu)$, and the second is the corollary of the continuity equation and of the equation for div$(\varepsilon\mathbf{E})$. The boundary conditions for equations (1) arise from the equality to zero of the normal component of the conduction current at the object's boundary: $\mathbf{n} \cdot \mathbf{E} = 0$, where $\mathbf{n}$ is the unit vector normal to the object's surface. Suppose that the medium acts to cause a slight change in the inductor's field specified by the magnetic vector potential $\mathbf{A}_0$ and $\mu = 1$. Then equations (1) may be approximately replaced by an equation of the form

$$\nabla^2\mathbf{A} = \frac{4i\pi\omega}{c^2}\left(\sigma + \frac{i\omega}{4\pi}\varepsilon\right)\mathbf{A}_0. \qquad (2)$$

It describes the magnetic field set up by the induced currents and displacement currents brought on to flow in the medium by the alternating magnetic field of the inductor. As equation (2) implies, the induced current proportional to the conductivity of the medium contributes to the magnetic field's quadrature component shifted through $\pi/2$, relative to the inductor's field, and the displacement current proportional to the permittivity contributes to the in-phase quadrature component.

By varying the two quadrature components of the detector signal, it is possible to independently determine the integral conductivity and permittivity of the medium. Importantly, the task of finding the conductivity is facilitated, because in the absence of a medium the quadrature component is zero, and the accuracy of measurement is limited solely by the absolute accuracy of the recorder. In contrast, in order to determine the permeability, one needs to measure small changes in the in-phase quadrature component in the presence of a strong inductor signal, so such measurements are, of course, less accurate. It is likewise clear why difficulties arose in [6] and [7] in the attempts to visualize the distribution of electric conductivity from measurements of the total amplitude of the magnetic field—in a linear approximation the conducting medium affects only the phase of the observed field. Equation (2) might be used to approximately solve the inverse problem of image reconstruction. From a practical point of view, however, it appears more attractive to use a method in which the system is treated in a quasi-static approximation and resort is made to equivalent circuits.

In a quasi-static approximation ($\omega \ll 2\pi c/l$, where l is the interturn spacing) in free space, the system may be treated as an air-core transformer. The inductor is traversed by current I_{ind}, which lags $\pi/2$ behind voltage U_{ind}, whereas no current is flowing in the detector (the indicator is assumed to have an infinite input impedance). In the absence of conducting objects in the surrounding space and on neglecting the resistance of the inductor and the displacement current, the indicator will measure a voltage U_{det} in phase with U_{ind}, whose amplitude is $U_2 = M_{12}U_1/L_1$, where L_1 is the self-inductance of the turn and M_{12} is the mutual inductance of the turns. Inductive coupling means that some of the magnetic flux produced by the inductor threads the detector turn and create an emf of induction there. Thus, the inductor and the detector are coupled solely by lines of magnetic flux $\mathbf{B}$ threading the two turns. In the space between the turns, the lines are drawn into a beam whose diameter is not greater than that of a turn (see Fig. 1). Now suppose that a small, weak conductor or magnetic object is placed in the space between the turns. Induced and displacement currents will now exist in the object or it will be magnetized, thus changing the magnetic field. If the magnetic field preserves its geometry, the detector signal would be changed only if the object crossed this narrow beam of lines of magnetic flux (the common magnetic flux of the two turns). This change would be greater, the greater the extent of the object along the beam. This suggests an analogy with X-ray tomography, except that the straight beam of X-rays is replaced by a curved beam of force lines.

Unfortunately, a quasi-static electromagnetic field strongly differs from short-wave (high-frequency) radiation. As the equation div$\mathbf{B} = 0$ suggests, there is no way of changing the magnetic field in a local beam of force lines without a change in the geometry and intensity of the field around the beam. That is, the object will change the field both in- and outside the beam it traverses; an object outside the beam that couples the detector and inductor will affect the detector signal. Nevertheless, the analogy with X-ray tomography does make some sense. The point is that the region where each probe or search coil has the highest intensity coincides with the beam of force lines that couple the coil and the inductor, and the nonlocal character of interaction between the object and the field only limits the resolving power of the system.

For back projection along the unperturbed lines of the magnetic field to be possible, it is essential that the perturbations introduced by the test medium be small. That is, measurements should be taken under conditions of a weak skin effect: $\delta \gg l$, where δ is the skin depth for the magnetic field in the test medium. On the other hand, the influence of the test medium on the magnetic field should be strong enough to be sensed by the detector. The above conditions are the criteria for the choice of the operating frequency ω for the tomograph. In contrast to an electric-impedance tomograph, it is possible, through an appropriate choice of frequency, to assure a linear approximation in the reconstruction of not only small changes in, but also the absolute values of, the object's conductivity. Also, because no electrodes need to be placed on the surface of the object, whose shape is not known in advance, it is possible to take highly accurate initial (reference) measurements in the absence of any body. A further distinction of a magnetic-induction tomograph, compared to its electric-impedance counterpart, is that its zones of maximum sensitivity are three-dimensional structures, or pipes, which couple the inductor and the detector. In an electric-impedance tomograph, they are spaces between two infinite surfaces—the equipotential surfaces of the electric field. Therefore, in a magnetic-induction tomograph, the influence of the objects located out of the test plane must be weaker than it is in an electric-impedance tomograph.

Consider the equivalent circuit of a system which consists of an inductor L_1 connected to a voltage source, a detector L_2, and a weakly conducting object placed between them (see Fig. 2). The model of the object is a transformer winding L_3 loaded into the parallel connection of a resistance $R \gg L_3\omega$ (the condition of the weak skin effect) and a capacitance $C \leq 1/\omega R$ (it is assumed that the displacement current in the object is not greater than the conduction current). By Kirchhoff's rules for harmonic currents, the equation for the complex amplitudes of circuit voltages and currents may be written as

$$\begin{aligned} U_1 &= i\omega(L_1 I_1 + M_{13} I_3), \\ U_2 &= i\omega(M_{12} I_1 + M_{23} I_3), \\ 0 &= \frac{R}{i\omega RC + 1} I_3 + i\omega(M_{13} I_1 + L_3 I_3), \end{aligned} \tag{3}$$

where U_i and I_i are the voltages across and the currents in the corresponding windings, respectively, L_i is the self-inductance, and M_{ij} is the mutual inductance (see Fig. 2). On neglecting the higher than first-order terms in the small parameter $\omega L_3/R$ and $\omega^2 L_3 C$, we find from equations (3) that the current in the inductor and the voltage across the detector are connected as

$$U_2 = \left[\omega M_{13} M_{23}\left(\frac{1}{R} + i\omega C\right) + iM_{12}\right]\omega I_1, \tag{4}$$

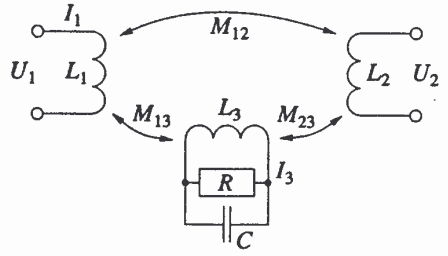

Fig. 2. Equivalent input circuits of a magnetic-induction tomograph.

and the voltages across the inductor and detector, as

$$U_2 = \left[M_{12} - i\omega M_{13} M_{23}\left(1 - \frac{M_{12} M_{13}}{M_{23} L_1}\right) \times \left(\frac{1}{R} + i\omega C\right)\right]\frac{U_1}{L_1}. \tag{5}$$

Two important things can be inferred from equations (4) and (5). First, in a linear approximation, as was to be expected from equation (2), the amplitude of the detector signal is independent of the conductivity, but does depend on the permittivity of the object. The conducting object acts to change the phase of the observed signal (the detector signal acquires a small quadrature component in phase with the current in the inductor). Measurement of a phase shift, which reduces to measuring time intervals and can be readily done to a high degree of accuracy, is preferable to measurement of quadrature signal amplitudes, as this would involve effort-consuming and inaccurate voltage–code conversions. Second, it is advisable to observe the change in the phase of the detector signal relative to that of the current in the inductor and not relative to the voltage across the inductor. In the latter case, the change in the phase is smaller, and the measured result can be strongly affected by objects situated close to the inductor and not necessarily inside the sensitivity zone of the detector. Moreover, such phase measurements are less sensitive to stray capacitive coupling and the permittivity of the object, because these two factors affect the amplitude more than the phase of the detector signal.

So let the phase shift between the current in the inductor and the voltage across the detector be $\Delta\varphi - \pi/2$. On putting $\Delta\varphi \ll 1$, which can be always arranged through an appropriate choice of frequency ω, we deduce from equation (4) in a linear approximation

$$\Delta\varphi = \frac{\omega M_{13} M_{23}}{M_{12} R}. \tag{6}$$

We now turn to determine the relation between the variables occurring in equation (6) and the characteristics of the test object. Let the object have an extent dl along the magnetic field and intercept all of the

magnetic flux common to the inductor and detector in the transverse direction. The resistance R seen by the displacement current induced by the magnetic field is inversely proportional to the cross section traversed by the current and the specific conductivity σ of the object. Hence, equation (6) may be recast as

$$d\varphi = \omega W \sigma dl, \quad (7)$$

where W is a geometric weight factor determined by the relative position of the inductor, object, and detector. From the same geometric considerations, the capacitance C of the test object can be assessed as being $\varepsilon W/4\pi$, and this estimate can advantageously be used in reconstructing the permittivity from the measured detector signal quadrature component in phase with the inductor current. Upon integrating equation (7) along the line of magnetic flux that couples the inductor and detector, we find for an extended medium that the measured phase shift $\Delta\varphi$ is equal to the linear integral of the weighted conductivity. With a set of such integrals for all inductors and detectors disposed along a closed contour around the test object, one is in a position to reconstruct the distribution of weighted conductivity over the cross section of the medium. In reconstructing, it is possible to apply the weight coefficient $1/W$ and thus to obtain the distribution of specific conductivity σ. Of course, the considerations drawn upon in deriving equation (7) are approximate. For example, the weight factor W will vary with the cross-sectional dimensions of the test object even if they are greater than the cross section of the magnetic flux common to the inductor and detector. Nevertheless, the relations and conclusions obtained above are sound enough to be used in designing a practical magnetic-induction tomograph and a workable conductivity reconstruction algorithm.

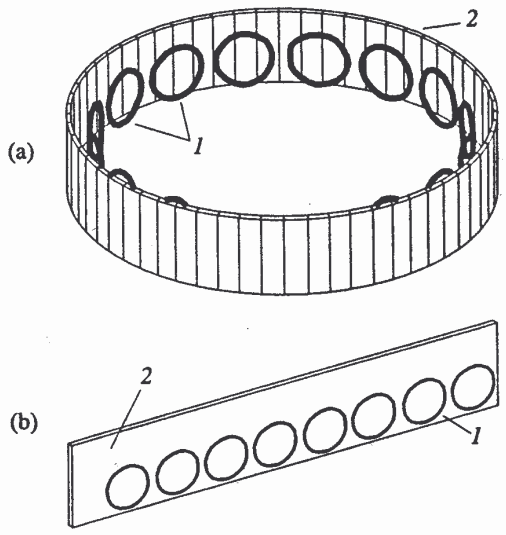

Fig. 3. Measuring system of a magnetic induction tomograph with (a) cylindrical and (b) linear geometry: *1*, inductor and detector coils; *2*, shield.

2. THE MEASURING SYSTEM OF A MAGNETIC-INDUCTION TOMOGRAPH

To gather data necessary for image reconstruction, a tomograph must contain an assortment of inductors and detectors placed in the test plane. In the simplest configuration, the inductor and detector coils would be arranged in a circle around the object (Fig. 3a). Generally, the same coils can be used as inductors and detectors in turn. However, the use of specialized coils all but removes the switching problems and assures the necessary impedance match, and, importantly, the inductor and detector coils may then have different numbers of turns. During a measurement, one inductor is activated and all the detectors are sampled. This procedure is repeated for all inductors. The initial phase shifts arising from delays in signal processing, the influence of structural components located in the field of the inductors, and the like are measured in the absence of a test object inside the operating zone of the tomograph and stored in memory. Initial phase shifts can also be measured or calculated for the test space filled by a homogeneous or inhomogeneous conducting medium, so that the quality of visualization can be improved by cancelling the background conductivity, or to obtain dynamic tomograms (visualization of changes in conductivity).

Lines of magnetic flux extend on either side of the inductor's plane and may thread irrelevant objects nearby, thus giving rise to an objectionable influence. To avoid this, the assemblage of inductors and detectors should be enclosed in a shield. At low frequencies (up to several megahertz), the best choice would be a ferromagnetic shield, which would provide a closed path for the inductor's lines of magnetic flux. At higher frequencies, the simpler and more efficient choice would be a conducting electromagnetic shield. In good conductors, the skin depth at frequencies of the order of 10 MHz is about 10 μm. That is, the magnetic flux does not practically penetrate the shield; rather, its lines bend and pass over the shield surface. As can be gathered from Section 1 and noting the electric conductivity of human tissues [2], the operating frequency for a medical magnetic-induction tomograph should be chosen in the range 10–20 MHz. In other applications of magnetic-induction tomography (geophysical prospecting, nondestructive testing of materials), the operating frequency would be lower.

By use of several contours with coils arranged one above another and by taking concurrent measurements at several sections, it is possible to construct a three-dimensional distribution of conductivity. In many tasks, a linear arrangement of inductors and detectors (see Fig. 3b) would be useful. In contrast to electric-impedance tomographs with such geometry, which is discussed in [8], the magnetic-induction technique

removes degeneration in planes passing through the inductor–detector line, and the tomograph is able to isolate in the medium a slice perpendicular to the coil plane. The depth of visualization would then be about half the length of the measuring strip. By using several strips (an array of coils), it is possible to reconstruct a three-dimensional distribution of conductivity under the surface.

3. IMAGE RECONSTRUCTION

In a linear approximation, the phase shifts measured by the measuring system of the tomograph are integrals of the weighted conductivity taken along the lines of magnetic flux that couple a given inductor and detectors. With such data available for all inductors arranged in a closed contour around the test object, the conductivity in a given slice of the object can be reconstructed using the convolution and back-projection method [1]. This method is widely used in electric-impedance tomography [9]. In magnetic-induction tomography, however, as can be inferred from equations (1) and (2), the observed data correspond to the distribution of conductivity and not of its gradient, as is in electric-impedance tomography. Therefore, in reconstructing, one ought not to skip the convolution stage (data filtering by a filter that has a ramp space–frequency response).

For a polar-geometry tomograph, the back-projection and weighting procedure can be formally described by a relation of the form

$$\sigma(r_0, \theta_0) = N\sum_{\theta_i} W(r_0, \theta_0 - \theta_i) \times \Delta\varphi(\theta_B(s, r_0, \theta_0 - \theta_i)|_{r_B(s, r_0, \theta_0 - \theta_i) = 1, s > 0} + \theta_i), \quad (8)$$

where σ is the specific conductivity of the medium at a point whose polar coordinates are (r_0, θ_0); θ_i is the polar angle of the inductor (the inductors and detectors are set up on a unit circle); $\theta_B(s, r, \theta)$ and $r_B(s, r, \theta)$ are the parametric equations of a line of magnetic flux for an inductor with $\theta_i = 0$ passing through the specified point (r, θ); s is the distance along the line from that point to the present point on the line; an increase in s corresponds to moving away from the inductor; N is a calibration coefficient; and $\Delta\varphi(\theta)$ is the phase that would be measured if the detector were located at point $(1, \theta)$.

Actually, the detectors are located at fixed points spaced a discrete step apart. Therefore, $\Delta\varphi(\theta)$ is calculated by linearly interpolating the indications of two detectors nearest to the required point. The weight coefficient W is chosen so that, for the same small test object, conductivity σ will be independent of its coordinates. To simplify the manipulations in determining the weight coefficient, the inductor and the detector may be approximated by point dipoles, and the test object, by an assemblage of dipoles arranged along a line perpendicular to the plane of visualization, such that the dipole moment of each dipole is proportional to the magnetic field of the inductor at the location of the dipole and is directed along that field. Equation (8) takes advantage of the fact that a system in which the inductors and detectors are arranged in a circle around the test object has the property of central symmetry. In that case, the weight factor W and lines of magnetic flux need to be calculated for only one inductor, and to pass to any other it would suffice to rotate the coordinate system through the required angle.

By an appropriate choice of the operating frequency for the tomograph, it is possible to assure the validity of the linear approximation used in image reconstruction. In some cases, however, a need may arise, as a way of enhancing the accuracy, to allow for the nonlinearity associated with the changes that the presence of the object makes in the geometry of the lines of magnetic flux. An image can then be reconstructed by successive iterations, in which case the magnetic field at a given iteration would be corrected according to the results of conductivity reconstruction at the previous iteration. As an alternative, image reconstruction in magnetic-induction tomography can use the inversion method. It is based on an expansion of the sought conductivity distribution into an orthogonal system of basis distributions, with the expansion coefficients calculated by a procedure that would minimize the difference between the results obtained by solving the direct problem [equation (1) or (2) for magnetic-induction tomography] and real measurements.

To test the possibility of obtaining images by magnetic-induction tomography, we have modeled the results measured by a tomograph with 32 inductors and detectors arranged in a circle around an object whose conductivity distribution over the cross section is shown in Fig. 4a. This distribution is assumed to model the cross section of the human rib cage. For magnetic-induction tomography, the direct problem in a linear approximation corresponds to equation (2). In the case of free space, this equation can be solved using Green's function, that is, the Biot–Savart–Laplace equation, where the current density is given by the right-hand side of equation (2). Taking as $\mathbf{A}_0$ the vector potential of the magnetic dipole that approximates the inductor and assuming that $\omega\varepsilon \ll \sigma$, the amplitude of the magnetic flux perturbation $\mathbf{B}_1$ produced by a conducting object may be written as

$$\mathbf{B}_1 = \frac{i\omega}{c^2}\int_V \sigma \frac{\mathbf{R} \times (\mathbf{m} \times \mathbf{R}_0)}{R_0^3 R^3} dV,$$

where $\mathbf{m}$ is the amplitude of the inductor magnetic moment, $\mathbf{R}_0$ is the radius vector from the inductor into dV, and $\mathbf{R}$ is the radius vector from dV to the observation point. The perturbations thus calculated determine the phase shifts of the signals sensed by the detectors, which were used as a reference to reconstruct the conductivity by the convolution and back-projection

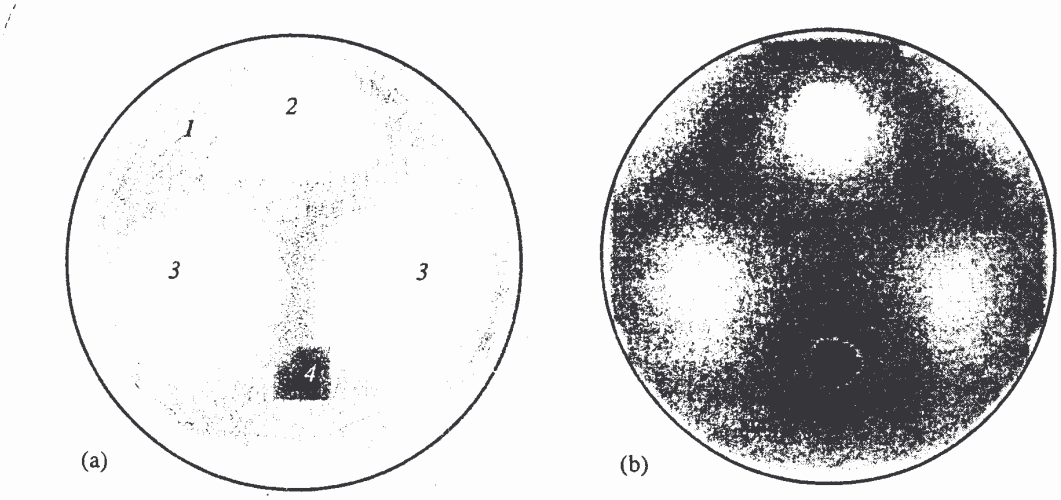

Fig. 4. (a) Initial electric conductivity distribution modeling the human rib cage and (b) its visualization by a magnetic-induction tomograph. The image has been reconstructed by the back projection method using calculated phase shifts: *1*, skeletal muscles (0.1 S/m); *2*, spine (0.007 S/m); *3*, lungs (0.05 S/m); *4*, heart (0.5 S/m).

method. For a high-quality reconstruction of the internal structure of extended conducting objects with a relatively small internal variation of conductivity, such as the human body, the phase shifts to be used as reference should be those corresponding to a body with a homogeneous conductivity only slightly different from the mean conductivity of the test body. Otherwise, the large phase shifts produced by the body would mask the small variations associated with its internal structure. The reconstruction thus obtained is shown in Fig. 4b.

CONCLUSION

Magnetic-induction tomography offers a way to visualize the distribution of conductivity and permittivity in an inhomogeneous medium. By sensing the phase shift between the current in the inductor and the voltage across the detector, a magnetic-induction tomograph is able to visualize to a high degree of accuracy the distribution of absolute electric conductivity inside various objects while using a relatively simple apparatus. As with other low-frequency electromagnetic systems, a magnetic-induction tomograph cannot have a high resolving power, but it has a number of other advantages to offer. Compared to electric-impedance tomography, one such advantage is the possibility of accurately visualizing the static distribution of electric conductivity, because the inductors and the detectors take up fixed positions in space. Another advantage is that the user is in a position to adjust, as required, the nonlinear relation between the electric conductivity of the medium and the electromagnetic field at the periphery of the test object through an appropriate choice of magnetic-field frequency. Still another important advantage is that weakly conducting shells are transparent to magnetic fields, so that an opportunity presents itself to investigate, say, the distribution and variation of the impedance in the brain of adult subjects. Moreover, no physical contact has to be maintained with the object, and no harm can thus be done to it. Coupled with the fact that the penetrating capacity of the magnetic field can be controlled through the choice of frequency, these features open up broad prospects for the use of magnetic-induction tomography not only in medicine, but also in safety systems, customs control, geophysics, and industry.

REFERENCES

1. Natterer, F., *The Mathematics of Computerized Tomography*, Chichester: Wiley, 1986. Translated under the title *Matematicheskie aspekty komp'yuternoi tomografii*, Moscow: Mir, 1990.
2. Barber, D.C. and Brown, B.H., *J. Phys. E: Sci. Instrum.*, 1984, vol. 17, no. 9, p. 723.
3. Korzhenevskii, A.V., *Proc. IX Int. Conf. Electrical Bioimpedance*, Heidelberg, 1995, p. 532.
4. Cherepenin, V.A, Korzhenevskii, A.V., Kornienko, V.N., *et al.*, *Proc. IX Int. Conf. Electrical Bioimpedance*, Heidelberg, 1995, p. 430.
5. Shinkarenko, V. and Kostromina, E., *Proc. IX Int. Conf. Electrical Bioimpedance*, Heidelberg, 1995, p. 476.
6. Yu, Z.Z., Peyton, A.J., Conway, W.F., *et al.*, *Electronics Lett.*, 1993, vol. 29, no. 7, p. 625.
7. Al-Zeibak, S., Goss, D., Lyon, G., *et al.*, *Proc. IX Int. Conf. Electrical Bioimpedance*, Heidelberg, 1995, p. 426.
8. Powell, H.M., Barber, D.C., and Freeston, I.L., *Clin. Phys. Physiol. Meas.*, 1987, vol. 8, suppl. A, p. 109.
9. Barber, D.C. and Seagar, A.D., *Clin. Phys. Physiol. Meas.*, 1987, vol. 8, suppl. A, p. 47.